Journal of Sciences, Islamic Republic of Iran 31(3): 221 - 231 (2020) http://jsciences.ut.ac.ir
University of Tehran, ISSN 1016-1104

Using Artificial Neural Network Modeling in Predicting the Amount of Methyl Violet Dye Absorption by Modified Palm Fiber

R. Andayesh[1,2*], M. Abrishamkar[1,2], H. Hodaee[1,2]

[1] *Department of Chemistry, Science and research Branch, Islamic Azad University, Ahvaz, Islamic Republic of Iran*
[2] *Department of Chemistry, Islamic Azad University of Ahvaz, Ahvaz, Islamic Republic of Iran*

Received: 26 July 2019 / Revised: 8 November 2019 / Accepted: 3 December 2019

Abstract

Bio-absorbent palm fiber was applied for removal of cationic violet methyl dye from water solution. For this purpose, a solid phase extraction method combined with the artificial neural network (ANN) was used for preconcentration and determination of removal level of violet methyl dye. This method is influenced by factors such as pH, the contact time, the rotation speed, and the adsorbent dosage. In order to find a suitable model of parameters and calculate the desired output, two radial basis function (RBF) and multi-layer perceptron (MLP) non-recursive functions, which are among widely used artificial neural networks, were used for training the input data. The performance of this method is tested by common statistical parameters including RMSE, MAE, and CE. The results show that the artificial neural network algorithm has a good performance in simulating and predicting the removal of violet methyl dye.

Keywords: Palm fiber; Violet methyl colour; Adsorbent; Neural network; Prediction.

Introduction

Chemical dyes are one big part of organic compounds that cause pollution in natural waters. These dyes are used for industrial and domestic purposes. Textile industry releases the highest amount of dye to the environment [1-3]. The use of dyes increases due to industrial development and growing demand for it. Methyl violet is a heterocyclic aromatic, odorless, solid compound that is soluble in water, ethanol, and di-ethylene glycol. The existence of this dye is dangerous for aquatic life because it is considered as mutagenic and mitotic poison, and thus carcinogenic. Removing methyl violet as an alkaline dye from the aqueous solution was investigated during the photo-catalytic reaction and Sono photo-catalytic by titanium dioxide (TiO_2) nanoparticles. Studies have shown that higher temperatures and lower initial concentration lead to higher removal rates. During recent years, various chemical methods have been developed to remove color dyes, including adsorption [4], Fenton process [5], photo/ferrioxalate system [6], and photo-catalytic and electrochemical combined treatments [7]. Adsorption is the result of the interaction of physical attraction forces between porous solid surfaces and molecules of substances taken from the fluid phase. Solid phase

* Corresponding author: Tel: +989120722359; Fax: +9842422435, Email: rashinandayesh@gmail.com

extraction and two beam spectrophotometer were used in this study. Various agricultural waste materials have been studied for the removal of different dyes from aqueous solutions at different operating conditions. Agricultural waste includes durian (*Durio zibethinus* Murray) peel [8], guava (*Psidium guajava*) leaf powder [9], peanut hull [10], *Citrullus lanatus*rind [11]. Palm fiber used in this study, is a chemically inert, non-toxic, biodegradable substance. This abundant renewable source is an agricultural byproduct that can be used as an absorbent for the removal of dyes from aqueous solutions. Through a process called activation, carbon-containing materials such as palm fiber are converted to activated carbon which is composed of a two phase process. The first step includes a pyrolysis of an agricultural by-products/wastes which increase the number of pores. While in second step, enlargement of pores in the carbonized material is achieved. In this study, activated carbons derived from palm fiber present comparable adsorption capacities which can be recommended as a suitable absorbent for methyl violet from textile wastewater. Besides, the adsorbed methyl violet can be easily extracted from adsorbent and there is no need to use a modifier to adjust the surface of the palm fibers. Furthermore, palm fibers can be used several times which in turn, shows the high performance of the method. The outstanding characteristic of the present study is using algorithms, artificial intelligence, and updated artificial neural network functions in anticipating the amount of determination and elimination of methyl violet dyes in the prepared sample solutions. In this process, after performing a few optimal tests, an algorithm can be created based on obtained data. Next, instead of doing test in other different circumstances, the removal percentage values can be predicted by the prepared artificial neural network algorithms. Reducing the cost of raw materials as well as reducing the use of expensive laboratory equipment and instruments can be noted as the advantages of this method. Also, the time of the analysis and interpretation can be considerably shortened using this method. In the present study, the ability of two common artificial neural network (ANN) functions (i.e., radial basis function, RBF, and multilayer perceptron, MLP) are assessed to predict the amount of removed dye. Finally, the performance of these artificial neural networks is tested by reliable statistics standards.

Materials and Methods

Materials used in this study include methyl violet dye with a molecular mass of 393.95, hydrochloric acid 37%, and sodium hydroxide, all produced by Merck Company (Germany) with high analytical purity. Furthermore, twice distilled water was used. The palm fiber prepared from palm trees of Jannat Makan village in the suburb of Gotvand city was used as an adsorbent.

About 1 cm glass cells for measuring the absorption and drawing the whole color solutions in λ= 581.6 nm and two beam spectrophotometer Lambda135 model made by Perkin-Elmer manufacturers were used in this study. A pH meter (F-11 model made by Horiba in Japan) was used to control the pH of aqueous solutions. For multiple stirring of the solution, a shaker (HS 501 digital) made by IKA-Werker in Germany was used. In order to weigh the studied samples, a balance BP210D (Sartorius Company, Switzerland) with a weighing capacity of 200 g and accuracy of 0.0001 was used. A centrifuge device made by Kokusan manufacturers in Japan was used for centrifuge tests. All Shushed balloons, volumetric flasks, pipettes, Erlenmeyer flasks, funnels, and glass stirrers were made of pyrex.

Preparation of samples for analysis

In the present study, palm fiber was prepared in winter from palm trees of Jannat Makan village, (in the suburb of Gotvand city in Khouzestan province, Iran). It was washed for several times by detergent and drinking water before using as a sorbent in order to remove dust and mud and was rinsed by distilled water for several times. Next, it was dried by the oven at 80 ℃ for 24 h. Dried palm fiber was crushed by gristmill (at different times of grinding to make different estimated sizes) to obtain modified palm fiber. The laboratory screening was used in various meshes (18, 25, 35, and 60) to obtain different particle sizes (0.25, 0.5, 0.1, and 0.75 mm). Afterward, 5 g of palm fiber was gradually added to 70 ml of concentrated hydrochloric acid in a 100 ml bécher to prepare modified palm fiber. To completely remove the excess acid, it was smoothened by thick filter paper after 2 h. After that, ethylene-diamine was added to a 30 ml volumetric flasks, and the adsorbent was filtered and washed by distilled water after 2 h until the leachate is a colorless and clear. Then, solid adsorbent on the filter paper was placed for 24 h on aluminum foil in the oven at 80 ℃ and was dried.

Static laboratory method

Static tests were conducted at 25 ℃ to remove methyl violet dye and to study the effect of important parameters including pH, the amount of adsorbent, the contact time, and stirring speed of solution. For this purpose, 50 ml of dye solution with concentrations of 100 and 200 ppm was added to a certain amount of palm fiber as an absorbent (0.1 g) and then was stirred in the shakers at a constant speed of 120 rpm. Samples

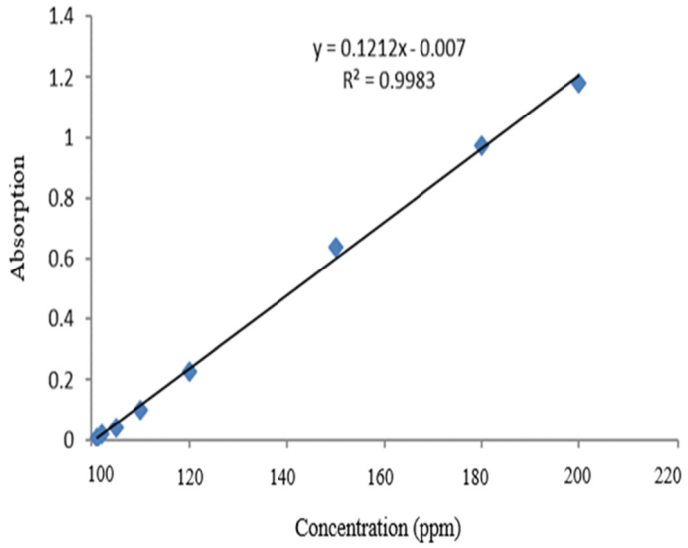

Figure 1. Calibration curve to determine the concentration of methyl violet color

were centrifuged for 15 min at different time intervals. In order to determine the residual concentration of methyl violet colour, the adsorption of the top layer of solution was measured by UV-Vis in λ = 581.6 nm. Figure 1 represents a calibration curve for methyl violet concentration in the range of 100-200 ppm and the amount of absorbed dye was obtained using Eqn. (1):

$$qe = \frac{(C0-Ce)V}{W} \quad (1)$$

where C_0, C_e, V, and M are the initial concentration of dye in the solution (mg/ L), the balance concentration of dye (mg/ L), the volume of the solution (L), and the amount of adsorbent (g), respectively. At all stages of the investigation, the dye removal rate was obtained by Eqn. (2):

$$\text{Re}\,moval(\%) = (\frac{C_0 - C_e}{C_0}) \times 100 \quad (2)$$

General procedure

The column method was used because it is simple, more convenient, and requires no stirring. Besides, it is more efficient and economical in the industry. For this purpose, 0.1 g of modified palm fiber was spilled at the bottom of the column including a hopper bottom of the pack, to which 50 ml of methyl violet dye solution with 100 mgL^{-1} of concentration was added. Then, 50 ml of methyl violet dye was eluted for 60 min followed by measuring the absorbance of the solution.

Artificial neural network (ANN)

Artificial neural networks (ANNs) consist of simple operating units (neurons) that are connected in parallel. Once an artificial neural network (ANN) is trained, entering a particular input leads to a specific response. The network works based on the correspondence between the input and target so that the outputs of network and objective coincide.

Artificial neural networks (ANNs) are utilized in several applications including aerospace, transportation, banking, defense, electronics, entertainment, finance, industry, insurance, manufacturing, medical, petroleum, robotics, speech, security, and telecommunications. Figure 2 shows the overall performance of the neural network which is taken from the user's guide (Neural network Toolbox) [12]. Artificial neural network (ANN) generally provides better performance compared with the conventional modeling methods. Khajeh et al. [13], applied a low-cost adsorbent for the removal of manganese and cobalt ions from water samples and solid phase extraction of waste tea using flame atomic absorption spectroscopy (FAAS). They benefited the surface response idea and artificial neural network for modeling the removal of cobalt and manganese. The correlation coefficient for surface response and artificial neural network methods was calculated 0.944 and 0.902 for manganese and 0.942 and 0.912 for cobalt, respectively.

Spanila et al. [14] used a combination of experimental design method and artificial neural

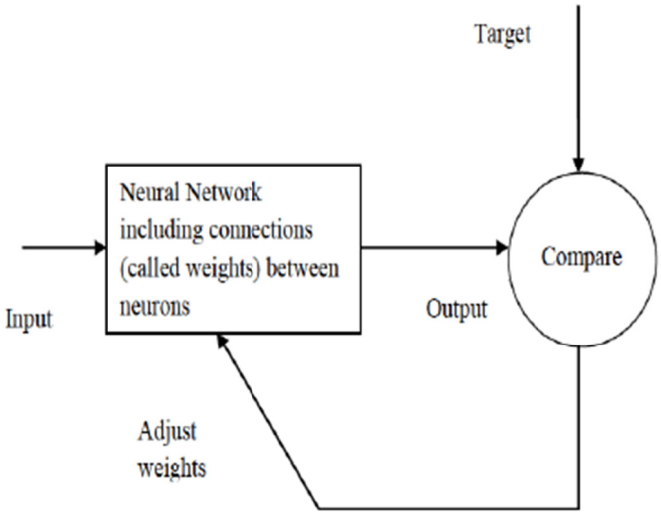

Figure 2. Schematic of the performance of the ANNs

network (ANN) to increase the effectiveness of resveratrol extract. They found that using the mentioned method, the number of performed tests reduce to less than half and, subsequently, the operation time of the data will decrease. The detection limit for prepared samples has been reported at 0.26 mgL^{-1}.

Radial basis function (RBF)

Radial basis function (RBF) networks are a subset of leading intelligent networks that employ advanced algorithms to train a network. They usually consist of a single hidden layer in which the activation function is known as a basis function. The radial basis function (RBF) networks have better performance from different aspects compared to back-propagation networks. Radial networks are faster than back-propagation networks and, because of their hidden layers' treatment, are less sensitive to input heterogeneous data network. The radial basis function (RBF) networks were introduced for the first time as a solution for multivariate linear problems by Moody et al. [15] and Broomhead and Lowe [16]. Radial basis function is one type of non-recursive neural network functions that easily solve the complex problems by simulating the human brain. Radial basis function clarifies the complex relationships between input and output data during the optimization process. The newrb function helps the radial basis functions to accurately predict output data through the network training by teaching points. Newrb adds neurons into the hidden layer until mean squared error (MSE) reaches the target. This command creates a two-layer network. The first layer contains neurons of the radial basis transfer function. In this layer, input weights are calculated by Euclidean distance of weighting function and its input data are multiplied by the network input functions. The second layer consists of neurons of the linear transfer function and the input weight are obtained by the dot product of the weight function and the input of the network plus the network input function [17].

Figure 3 shows a radial basis function structure with j input data. It consists of three layers including an input layer that receives input nodes as P_1, P_2, …, P_j, output layer that consists of linear activation function and network's outputs as Y_1, Y_2, …, Y_j, and a hidden layer containing radial basis transfer functions.

Levenberg-Marquardt function (LM)

The Levenberg-Marquardt function can be considered as the modified model of the Gauss-Newton process in which the parameters of the optimization process can be set [18,19]. Levenberg-Marquardt (LM) algorithm is known as a combination of the gradient reduction and Gauss-Newton methods, which is an effective optimization algorithm in controlling the operational process and mathematical modeling. This algorithm, which was suggested by Levenberg and then optimized by Marquardt, is used to solve nonlinear algebraic equations [20]. The Levenberg-Marquardt (LM) algorithm has been applied widely in solving inverse problems [21-24]. In general, a trained LM has a satisfactory generalized capability in mapping input patterns into target estimation [25-29]. Multilayer perceptron (MLPs) include an input layer, an output

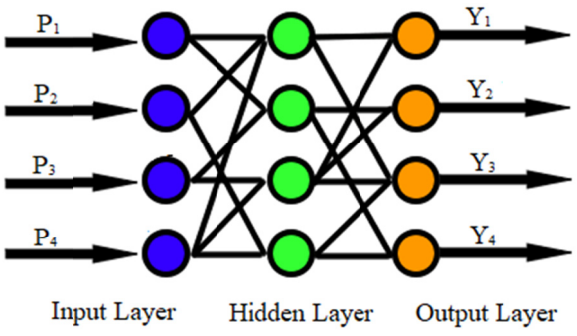

P1: pH
P2: Contact time
P3: Rounds of the shaker
P4: Adsorbent dosage

Figure 3. The schematic of the RBF's structure

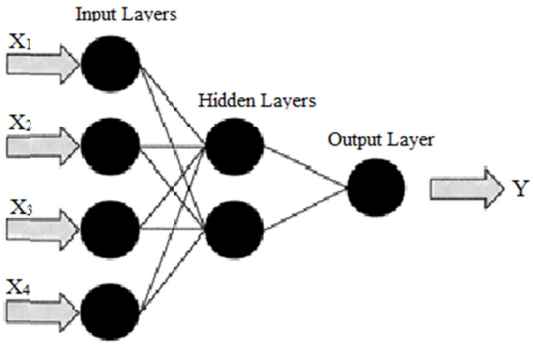

X1: pH
X2: Contact time
X3: Rounds of shaker
X4: Adsorbent dosage

Figure 4. Schematic of LM diagram with four groups of input data, one hidden layer, and an output data

layer, and at least one hidden layer with nonlinear processing units [30,31]. Figure 4 represents a diagram of Levenberg- Marquardt diagram with four groups of input data, one hidden layer, and an output data.

Methodology

Two neural network functions, radial basis function (RBF) and multilayer perceptron (MLP), were used in this study to train the input data and determine an algorithm for calculating the amount of violet methyl dye removal as an output data of neural network. Four types of input data were selected for training the neural network; i.e., pH, the contact time in a minute, the number of rounds of shaker in rpm, and the absorbent dosage in gL^{-1}. Network output is the amount of violet methyl colour removal existing in the sample solution. After proper training of network and obtaining appropriate algorithm of the neural network, input data of the test, which their output was measured and imported into the network in order to measure the efficiency of the algorithm in dye removal. The number of calibration data is 135 that form a 5×27 network. There are 27 rows that 20 of them were used for training the neural network and 7 of them were randomly used to test the calculation algorithm of the network.

The more uncertainty, mean absolute error (MSE), and standard error of under considered parameters are closer to 0, the higher the performance of the designed artificial neural network is for predicting the test data. For an efficient artificial neural network algorithm, the

coefficient of determination (R^2), which has a range of 0 to 1, is close to 1. If this parameter is 1, there will be a perfect correlation between measured and predicted data. On the other hand, if the coefficient of determination is 0, the regression equation cannot help to predict values.

Results and Discussion

Several factors were investigated to obtain optimum conditions for removal of violet methyl dye. To study the effect of pH on the amount of adsorbed dye, 50 ml of colour solution with 100 mg/L of concentration was spilled to 10 Erlenmeyer flasks. Then pH solution was adjusted by NaOH and HCl, and 0.0744 g of adsorbent size 0.25 was added to each flask and was stirred on a shaker at around 120 rpm for 30 min. The solution was cleared and then the absorption was read at the maximum wavelength in 581.6 nm. Selected ranges were chosen for other parameters affecting the dye removal, including the number of shaker rounds, the contact time with the adsorbent, and the adsorbent dosage. The training and test data are shown in Table 1 and 2, respectively.

Table 1. Experimental data for training an ANN model

Run	Adsorbent dosage (g/L)	pH	Time (min)	Rotation speed (rpm)	Real output percent
1	1.2	9.5	50	80	88.41
2	1.2	11	30	80	83.7
3	0.4	9.5	50	100	60.93
4	1.2	11	10	100	79.95
5	2	9.5	30	80	95.64
6	1.2	9.5	30	100	78.01
7	1.2	9.5	50	120	91.32

Table 2. List of data for test and validation of the designed ANN algorithms

Run	Adsorbent dosage (g/L)	pH	Time (min)	Rotation speed (rpm)	Real output percent
1	0.4	8	30	100	62.33
2	0.4	11	30	100	66.38
3	2.0	8	30	100	92.96
4	2.0	11	30	100	90.78
5	1.2	9.5	10	80	71.16
6	1.2	9.5	10	120	80.86
7	1.2	8	30	80	87.25
8	1.2	8	30	120	87.00
9	1.2	11	30	120	90.10
10	0.4	9.5	10	100	57.59
11	2.0	9.5	10	100	83.70
12	2.0	9.5	50	100	97.32
13	1.2	8	10	100	72.61
14	1.2	8	50	100	87.38
15	1.2	11	50	100	90.20
16	0.4	9.5	30	80	59.86
17	0.4	9.5	30	120	69.80
18	2.0	9.5	30	120	96.52
19	1.2	9.5	30	100	79.46
20	1.2	9.5	30	100	79.54

Statistical diagram of neural network evaluation

The output charts for this session are shown in Figure 5. As can be seen, training data in both methods, i.e., the radial basis function (RBF), and multilayer perceptron (MLP), have less distribution of determined linear regression than the testing data. Also, the data deviation from the regression line for radial basis function (in both training and test data sets) is less than the amount of multilayer perceptron function, suggesting the higher performance of radial basis function algorithm.

Figure 6 presents how the actual data obtained from experiments are consistent with those predicted by the neural network for training and testing data. As can be noticed, the results of the artificial neural network (ANN) can predict the specifications of the aerodynamic probe with an appropriate accurately. Matching between actual and predicted data is quite satisfactory for both functions but the performance of radial basis function (RBF) is higher.

The absolute error using the neural network for training and testing data is presented in Figures 7a and 7b and Figure 7c, respectively. When training the radial basis function (RBF), the maximum absolute error is equal to 0.3491 and its minimum value is 3.21E-07. Minimum and maximum absolute errors in the training data by multilayer perceptron (MLP) function are

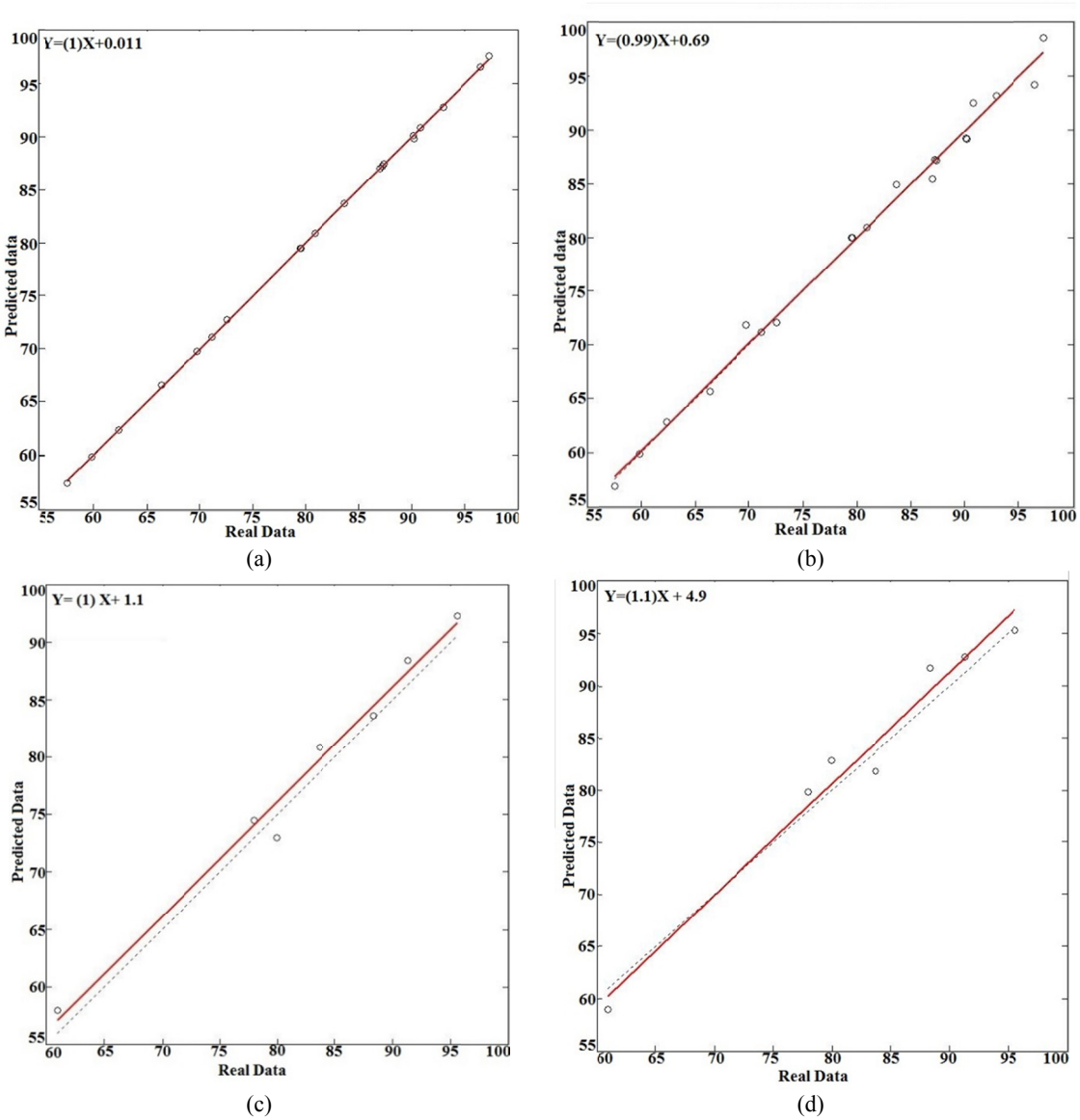

Figure 5. Regression line for performance of neural network model: RBF (a) train data; (c) test data; Levenberg-Marquardt function (b) train data (d) test data

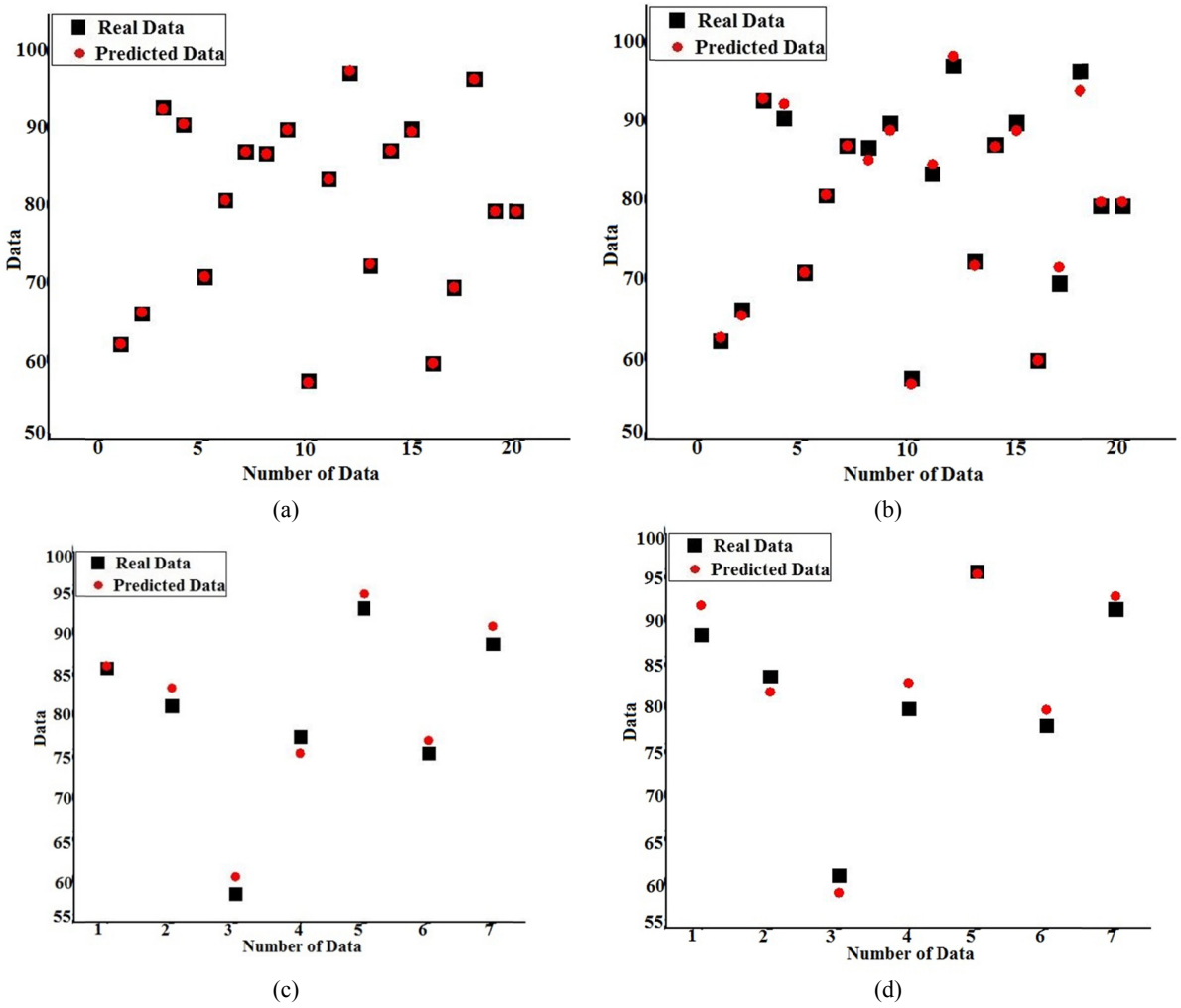

Figure 6. Point adaption graph of predict and real data: RBF (a) train data; (c) test data; Levenberg-Marquardt function (b) train data (d) test data

2.3648 and 1.06E-08, respectively. Maximum and minimum absolute errors for predicting the test data for radial basis function (RBF) and multilayer perceptron (MLP) are (2.1938 and 0.2680) and (3.3624 and 0.3089), respectively. To determine and test the performance of functions, neural network efficiency should be evaluated. Several statistical parameters are used for this purpose. Root mean squared error (RMSE) (uncertainty), mean absolute error (MAE), and the coefficient of efficiency (CE) are some of these parameters, which are calculated as Eqns. (3) to (5), respectively [32-38].

$$RMSE = \left[\frac{1}{N}\sum_{i=1}^{N}\left(\hat{u}_i - u_i\right)^2\right]^{1/2} \quad (3)$$

$$MAE = \frac{1}{N}\sum_{i=1}^{N}\left|\hat{u}_i - u_i\right| \quad (4)$$

$$CE = 1 - \frac{\sum_{i=1}^{N}\left(\hat{u}_i - u_i\right)^2}{\sum_{k=1}^{N}\left(\hat{u}_i - \bar{\hat{u}}\right)^2} \quad (5)$$

The higher the uncertainty level is, the closer the mean absolute error (MAE) and the coefficient of efficiency (CE) of the considered parameter are to 0, and thus the designed neural network will better predict the test data. For a suitable artificial neural network (ANN) algorithm, the coefficient of determination (R^2)

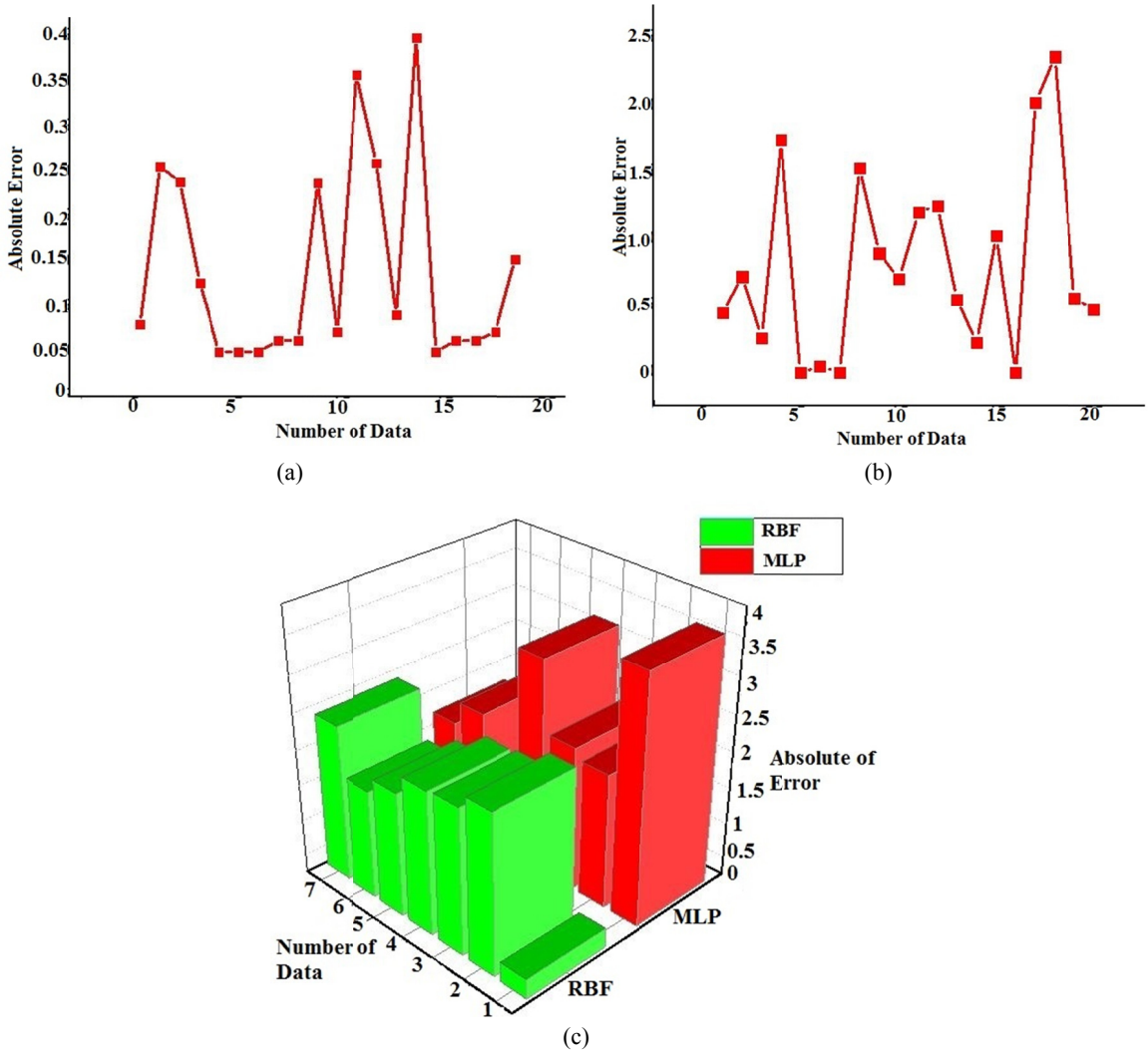

Figure 7. The absolute error of ANNs: train data (a) RBF (b) and Levenberg-Marquardt functions; (c) test data for RBF and Levenberg-Marquardt functions

is close to 1.

The results of the statistical parameters for measuring the performance of multilayer perceptron (MLP) and radial basis function (RBF) algorithms are presented in Table 3. As can be seen, for both training data and test data, the uncertainty level and mean absolute error (MAE) for the radial basis function (RBF) algorithm are closer to 0 and the correlation coefficients are closer to 1. Therefore, this model has a higher performance in the removal of violet methyl dye.

Evaluating real samples

In order to evaluate the performance of the method, some real water samples from the tap water, Karun water, Karkheh dam water, and Ramak Company sewage were prepared. Methyl violet concentration was

Table 3. Statistical parameters for evaluation of efficiency of MLP and RBF functions

Function	Algorithm	Statistical parameter		
		Uncertainty	Mean absolute error	Coefficient efficiency
Train Data	RBF	0.140415	0.001517093	0.999863
	MLP	1.069576	0.022450038	0.992082
Test Data	RBF	1.795902	0.03829	0.971527
	MLP	2.161749	0.480348477	0.964196

100-200 ppm and the adsorption capacity ranged from 96.10 to 96.66 mg g^{-1} for tap water, from 96.31 to 96.40 mg g^{-1} for Karun water, from 96.25 to 96.33 mg g^{-1} for Karkheh dam water, and from 95.32 to 96.55 mg g^{-1} for Ramak Company sewage. Based on the results, water purified with this method can be reused in industries. In addition, the adsorption capacity of methyl violet was found to be more dependent on pH and the adsorbent dosage. The adsorption capacity increased sharply by enhancing the adsorbent dosage but it remained constant at the concentration of 0.1 mg g^{-1}. As demonstrated, time of stirring and the number of shaker rounds are important variables in determining methyl violet adsorption capacity. Therefore, these variables were chosen to be the input parameters of the computational the artificial neural network models.

Conclusions

In this study, bio-absorbent palm fiber was applied for removal of cationic violet methyl dye from water solution and simulating it using the artificial neural network (ANN). Based on different experimental conditions, a suitable artificial neural network (ANN) algorithm was achieved accordingly. The performance of two artificial neural network functions (i.e., RBF and MLP) were evaluated by statistical parameters and found that the radial basis function (RBF) has a higher ability in the removal of violet methyl dye compared to multilayer perceptron (MLP) non-recursive function. The advantages of using a neural network in the above method are reducing the examination time, reducing the costs, and decreasing the use of required laboratory samples.

References

1. Šmelcerović M., Đorđević D., Novaković M., Mizdraković M. Decolorization of a textile vat dye by adsorption on waste ash. J. Serb. Chem. Soc. **75**: 855–872 (2010).
2. Kim S., Lee Y.G., Jerng D.W. Laminar film condensation of saturated vapor on an isothermal vertical cylinder. Int. J. Heat Mass Transfer. **83**: 545-551 (2015).
3. Sharma P., K.Saikia B., R.Das M. Removal of methyl green dye molecule from aqueous system using reduced graphene oxide as an efficient adsorbent: kinetics, isotherm and thermodynamic parameters. Colloids Surf A Physicochem Eng Asp. **457**: 125–133 (2014).
4. Tan I.A.W., Hameed B.H., Ahmad A.L. Equilibrium and kinetic studies on basic dye adsorption by oil palm fibre activated carbon. Chem Eng J. **127**: 111–119 (2007).
5. Behnajady M.A., Modirshahla N., Ghanbary F. A kinetic model for the decolorization of C.I. Acid yellow 23 by Fenton process. J Hazard Mater. **148**, 98–102 (2007).
6. Huang Y.H., Tsai S.T., Huang Y.F., Chen C.Y. Degradation of commercial azo dyes reactive Black in photo/ ferrioxalate system. J Hazard Mater. **140**: 382–388 (2007).
7. Neelavannan M.G., Revathi M., Ahmed Basha C. Photocatalytic and electro-chemical combined treatment of textile wastewater. J Hazard Mater. **149**: 371–378 (2007).
8. Hameed B.H., Hakimi H. Utilization of durian durio zibethinus murray peel as low cost adsorbent for the removal of methylene blue from aqueous solution. Biochem Eng J. **39**: 338–343 (2008).
9. Ponnusami V., Vikiram S., Srivastava S.N. Guava Psidium guajava leaf powder: novel adsorbent for removal of methylene blue from aqueous solutions. J Hazard Maters. **152**: 276–286 (2008).
10. Tanyildizi M.S. Modeling of adsorption isotherms and kinetics of reactive dye from aqueous solution by peanut hull. Chem Eng J. **168**: 1234–1240 (2011).
11. Bharathi K., Suyamboo A., Ramesh S.T. Equilibrium, thermodynamic and kinetic studies on adsorption of a basic dye by Citrullus lanatus rind. Iran J Energy Environ. **3**, 23–34 (2012).
12. Çetintaş S., Bingöl D. Optimization of Pb(II) biosorption with date palm (Phoenix Dactylifera L.) seeds using response surface methodology. J. Water Chem. Technol. **40**: 370-378 (2018).
13. Khajeh M., Sarafraz-Yazdi A., Fakhrai Moghadam A. Modeling of solid-phase tea waste extraction for the removal of manganese and cobalt from water samples by using PSO-artificial neural network and response surface methodology. Arabian J.Chem. **10**: S1663-S1673 (2017).
14. Spanila M., Pazourek J., Farková M., Havel J. Optimization of solid-phase extraction using artificial neural network in combination with experimental design for determination of resveratrol by capillary zone electrophoresis in wines. J. Chromatogr. A. **1084**: 180–185 (2005).
15. Moody J., Darken C.J. Fast learning in networks of locally-tuned processing units. Neural Computation. **1**: 281-294 (1989).
16. Broomhead D.S, Lowe D. Multivariable functional interpolation and adaptive networks. Complex Syst. **2**: 321-355 (1988).
17. Eftekhari Zadeh E., Feghhi S.A.H., Roshani G.H., Rezaei A. Application of artificial neural network in precise prediction of cement elements percentages based on the neutron activation analysis. Eur. Phys. J. Plus. **131**: 167 (2016).
18. Levenberg K. A method for the solution of certain non-linear problems in least squares. Quart. Appl. Math. **2**: 164–168 (1944).
19. Marquardt D.W. An algorithm for least-squares estimation of nonlinear parameters. J. Soc. Ind. Appl. Math. **11**: 431–441 (1963).
20. Fan J.Y., Yuan Y.X. On the quadratic convergence of the Levenberg-Marquardt method without

nonsingularity assumption. Computing. **74**: 23–39 (2005).
21. Fan J., Pan J. A note on the Levenberg-Marquardt parameter. Appl. Math. Comput. **207**: 351–359 (2009).
22. Gavin H.P., Yau S.C. High-order limit state functions in the response surface method for structural reliability analysis. Structural Safety. **30**: 162-179 (2008).
23. Amini K., Rostami F. Three-steps modified Levenberg–Marquardt method with a new line search for systems of nonlinear equations. J. Comput. Appl. Math. **300**: 30–42 (2016).
24. Azimi A., Farhanieh B., Hannani S. Implementation of geometrical domain decomposition method for solution of axisymmetric transient inverse heat conduction problems. Heat Transfer Eng. **29**: 255–271 (2008).
25. Zhang N., Duan Z., Tian C. A complete axiom system for propositional projection temporal logic with cylinder computation model, Theor. Comput. Sci., **609**: 639–657 (2016).
26. Mu H., Li J., Wang X., Liu S. Optimization based inversion method for the inverse heat conduction problems. In. IOP Conference Series: Earth and Environmental Science, Ordos, China. **64**: no. 012094 (2017).
27. Czel B., Grof G. Inverse identification of temperature-dependent thermal conductivity via genetic algorithm with cost function-based rearrangement of genes. Int. J. Heat Mass Transfer. **55**: 4254–4263 (2012).
28. Liu F.B. Particle swarm optimization-based algorithms for solving inverse heat conduction problems of estimating surface heat flux. Int. J. Heat Mass Transfer. **55**: 2062–2068 (2012).
29. Paulsen B.T., Bredmose H., B.Bingham H. An efficient domain decomposition strategy for wave loads on surface piercing circular cylinders. Coast Eng. **86**: 57-76 (2014).
30. Eftekhari M., Yadollahi A., Ahmadi H., Shojaeiyan A., Ayyari M. Development of an artificial neural network as a tool for predicting the targeted phenolic profile of grapevine (Vitis vinifera) foliar wastes. Front Plant Sci. **9**: 1–10 (2018).
31. Duda P. A general method for solving transient multidimensional inverse heat transfer problems. Int. J. Heat Mass Transfer. **93**: 665-673 (2016).
32. Liu C.S., Chang C.W. Nonlinear problems with unknown initial temperature and without final temperature, solved by the GL (N, R) shooting method. Int. J. Heat Mass Transfer. **83**: 665–678 (2015).
33. Agha S.R., Alnahhal M.J. Neural network and multiple linear regression to predict school children dimensions for ergonomic school furniture design. Appl Ergon. **43**: 979–984 (2012).
34. Mustafa M.R., Rezaur R.B., Rahardjo H., Isa M.H. Prediction of pore-water pressure using radial basis function neural network. Eng. Geol. **135-136**: 40-47 (2012).
35. Santos R.B., Bonzi S.J., Rupp M., Fileti A.M.F. Comparison between multilayer feedforward neural networks and radial basis function network to detect and locate leaks in a pipeline transporting gas. Chem. Eng. Trans. **32**: 1375-1380 (2013).
36. Fan H.Y., Lu W.Z., Xi G., Wang S.J. An improved neural-network-based calibration method for aerodynamic pressure probes. J. Fluids Eng. **125**: 113-120 (2003).
37. Wu D., Warwick K., Ma Z., Burgess J.G., Pan S., Aziz T.Z. Prediction of Parkinson's disease tremor onset using radial basis function neural networks. Expert Syst Appl. **37**: 2923–2928 (2010).
38. Fan M., Li T., Hu J., Cao R., Wei X., Shi X., Ruan W. Artificial neural network modeling and genetic algorithm optimization for cadmium removal from aqueous solutions by reduced graphene oxide-supported nanoscale Zero-Valent Iron (nZVI/rGO) composites. Materials (Basel). **10**: 544-566 (2017).